Complexes of Functionalised Phosphine Ligands. Part 1. Complexes of Fe^{III}, Co^{III}, Ni^{II} and Re^{V} with Tridentate Schiff Bases having PNO, NNO and NNS Donor Sets. Crystal Structures of 2-$(Ph_2PC_6H_4N{=}CH)C_6H_4OH$ and $[Co\{2\text{-}(Ph_2PC_6H_4CH{=}N)C_6H_4O\}_2][PF_6]$†

Jonathan R. Dilworth,*[a] Stuart D. Howe,[a] Antony J. Hutson,[a] John R. Miller,[a] Jack Silver,[a] Russell M. Thompson,[a] Mary Harman[b] and Michael B. Hursthouse[b]

[a] *Department of Chemistry and Biological Chemistry, University of Essex, Wivenhoe Park, Colchester CO4 3SQ, UK*

[b] *Department of Chemistry, University of Wales, Cardiff CF1 3TB, UK*

The Schiff bases 2-$[Ph_2P(CH_2)_nN{=}CH]C_6H_4OH$ (n = 3, HL^1 or 2 HL^2), 2-$(RCH{=}N)C_6H_3(OH)X$-4 (R = 2-$Ph_2PC_6H_4$, X = H HL^3; R = 2-C_5H_4N, X = H HL^4; R = 2-C_5H_4N, X = Cl HL^5) were synthesised from the appropriate amine and aldehyde. On deprotonation these all functioned as tridentate monoanionic ligands to give complexes $[FeL_2]^+$ and $[CoL_2]^+$ with Fe^{III} and Co^{III} and neutral complexes of stoichiometry NiL_2 with Ni^{II}. The iron complexes were examined by Mössbauer spectroscopy which indicated the presence of two iron sites in $[FeL^1_2]^+$ with a spin-state equilibrium dependent on both temperature and the counter ion. The complex $[FeL^3_2]^+$ showed a single iron site, again with a spin state dependent on counter ion and temperature. The crystal structures of HL^3 and $[CoL^3_2]^+$ have been determined. The distortions in free HL^3 predispose it for co-ordination in a *fac* geometry to the Co with *cis*-PPh_2 groups, and the changes occurring on co-ordination are discussed in detail. Reaction of RCHO (R = 2-$Ph_2PC_6H_4$ or 2-C_5H_4N) with 2-aminobenzenethiol gave stable thiazoles $RCHNHC_6H_4S$-2 which did not ring open to give tridentate ligands even on reaction with base and/or metal ions.

There has been considerable recent interest in the chemistry of polydentate ligands with both hard and soft donor atoms, and we here report the synthesis and characterisation of transition-metal complexes of some monobasic tridentate Schiff bases containing PNO and PNS donor sets and a comparison with ligands containing NNO and NNS donor-atom sets. These were derived from 2-diphenylphosphinobenzaldehyde and pyridine-2-carbaldehyde respectively. The pyridyl-containing tridentate NNO compounds HL^4 and the 4-chloro-substituted HL^5 have been mentioned previously,[1] but detailed characterisation of these and their transition-metal complexes was not described. Whilst this manuscript was in preparation the synthesis of the PNO compound HL^1 and the rhenium(v) complex $[ReOCl_2L^1]$ was reported.[2] We include our synthesis and characterisation of the propylene-bridged derivative HL^1 and also that of the ethylene- and phenylene-bridged PNO analogues HL^2 and HL^3 respectively, together with a wider investigation of the chemistry of all these compounds with salts of the first-row transition metals Fe, Co and Ni and the third-row element Re. The crystal structure of HL^3 is reported and that of the complex $[CoL^3_2]^+$ is discussed in terms of the distortions occurring on co-ordination.

Results and Discussion

Synthesis and Properties of the Tridentate Schiff Bases.—The PNO-type Schiff bases HL^1 and HL^2 were prepared by treating the appropriate (aminoalkyl)diphenylphosphine with salicylaldehyde in ethanol under reflux. The PNO species HL^3 was similarly prepared from 2-(diphenylphosphino)benzaldehyde and 2-aminophenol. The yellow crystalline PNO Schiff bases resemble each other very closely in their chemistry as would be expected from their structural similarity. The full characterisation of these and other related species is given in the Experimental section, and the crystal structure of HL^3 was determined to investigate the changes occurring on co-ordination.

The NNO Schiff base was prepared as yellow needle-like crystals by condensation of 2-aminophenol with pyridine-2-carbaldehyde in methanol under reflux. HL^5 was prepared similarly using 5-chloro-2-hydroxyaniline, giving a deep orange crystalline product. The NNS species HL^6 was prepared from 2-acetylpyridine and 2-aminobenzenethiol, as a pale yellow crystalline solid. The potentially tridentate NNS donor base HL^8 was similarly prepared from 2-aminobenzenethiol and pyridine-2-carbaldehyde. All the Schiff bases are air stable both as solids and in solution, and show no signs of decomposition after standing in air for several months as judged by their IR and NMR spectra. The bases are soluble in a wide variety of common organic solvents [CH_2Cl_2, dimethylformamide (dmf), ethanol, methanol, acetone and tetrahydrofuran] and the IR spectra are unremarkable except for the characteristic (C=N) stretching band at about 1620 cm^{-1} and bands assigned to ν(OH), inferring that the Schiff-base form of the ligand predominates.

In the ^1H NMR spectrum of HL^1 the PCH_2CH_2 and PCH_2 protons appear as unresolved complex multiplets at δ 1.8 and 2.2 respectively. The NCH_2 protons give rise to a triplet at δ 3.6 ($^3J_{HH}$ = 6.4 Hz). The aromatic protons of the diphenylphosphino group and the salicylaldehyde aryl protons appear as a broad multiplet in the range δ 6.7–7.7. The CH=N proton is

† *Supplementary data available:* see Instructions for Authors, *J. Chem. Soc., Dalton Trans.*, 1994, Issue 1, pp. xxiii–xxviii.

Non-SI unit employed: $\mu_B \approx 9.27 \times 15^{24}$ J T^{-1}.

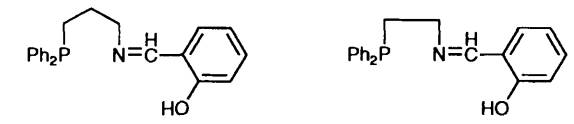

HL[1]

HL[2]

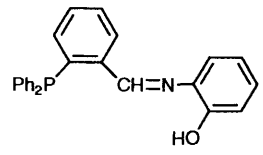

HL[3]

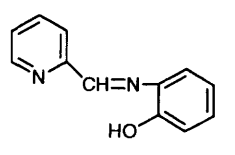

HL[4]

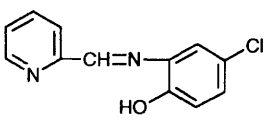

HL[5]

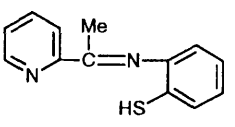

HL[6]

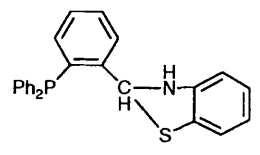

HL[7]

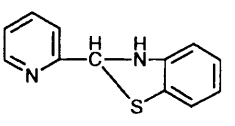

HL[8]

assigned to a singlet at δ 8.3. A broad singlet at δ 13.5 is assigned to the phenolic proton. The ^{1}H NMR spectrum of HL^2 is very similar to that of HL^1, but with unresolved multiplets centred at δ 2.7 and 3.9 assigned to the PCH_2 and NCH_2 protons respectively. The ^{1}H NMR spectrum of HL^3 is unremarkable and consists mainly of complex phenyl-proton resonances. However, the CH=N proton appears as a doublet at δ 9.03 due to coupling to P (J = 5.5 Hz). The ^{13}C-{^{1}H} NMR resonances exhibited by HL^1–HL^3 are as expected. The ^{31}P-{^{1}H} NMR spectra show the expected singlets at δ −15.7, −18.6 and −9.0 for HL^1, HL^2 and HL^3 respectively.

The IR and NMR data for the potentially tridentate NNS derivative HL^6 are consistent with the formation of the Schiff-base form $(C_5H_4N)CMe{=}NC_6H_4SH$. The formation of the ring-closed thiazole form $(C_5H_4N)CMeNHC_6H_4S$ is prevented, probably due to the steric effect of the methyl group on the imino carbon atom. The IR spectrum for HL^6 thus shows a weak broad band at 3150 cm^{-1} assigned to ν(SH) and a band at 1590 cm^{-1} assigned to ν(C=N). The attempted synthesis of a related 'Me-NNO' tridentate species from 2-acetylpyridine and 2-aminophenol was not successful. This is presumably because the formation of the Schiff base of the ketone is reversible, and sensitive to steric hindrance. The reaction of 2-(diphenylphosphino)benzaldehyde with 2-aminobenzenethiol in an attempt to make the PNS donor derivative ligand HL^7 did not give the Schiff-base form, but the much more stable five-membered thiazole ring structure $Ph_2PC_6H_4\overline{CHNHC_6H_4S}$. This is supported by IR and NMR data. Addition of an excess of base (either NEt_3 or NaOMe) and/or metal ions failed to open this apparently very stable thiazole form of this potentially tridentate ligand. This was confirmed by monitoring the reaction by ^{31}P NMR spectroscopy. The potentially tridentate NNS derivative HL^8 also exists in this very stable ring-closed thiazole form $(C_5H_4N)\overline{CHNHC_6H_4S}$ which similarly resists attempts to prepare transition-metal complexes, and reactions of either HL^7 and HL^8 with salts of Fe, Co and Ni lead to mixtures of impure products.

The structure of HL^3 is discussed together with that of $[CoL^3{}_2]^+$ below.

Synthesis and Characterisation of the Complexes.—The properties of the transition-metal complexes of the tridentate compounds are given in Table 1. The iron and cobalt complexes are synthesised by reaction of an ethanolic solution of the appropriate Schiff base in the presence of the base triethylamine with an ethanolic solution of either $FeCl_3$ or an aerated solution of $CoCl_2$. The cationic complexes of the type $[ML_2]^+$ (M = Fe or Co) are easily precipitated from solution in high yield as either hexafluorophosphate or tetraphenylborate salts, and readily recrystallised from dichloromethane–diethyl ether. All the iron and cobalt complexes except those of L^5 are soluble in a wide range of common organic solvents including CH_2Cl_2, ethanol and acetone, and insoluble in diethyl ether and light petroleum. Complexes of L^5 are extremely insoluble, due to the presence of the 4-chlorophenyl substituent. Reactions of the appropriate Schiff bases with $NiCl_2$ in ethanol yield neutral green or yellow solids analysing as $[NiL_2]$ which are extremely insoluble in common organic solvents including dmf and dimethyl sulfoxide (dmso), indicating the possible formation of oligo- or poly-meric species. Further detailed study of the nickel complexes was thus precluded by this insolubility. The neutral rhenium complexes are synthesised by refluxing an ethanolic solution of the Schiff base with $[NBu^n_4][ReOCl_4]$,[3] and analyse as $[ReOCl_2L]$. The rhenium complex with L^1 has been reported together with its crystal structure. It is soluble in dichloromethane, dmf and dmso.

All the complexes are air stable both as solids and in solution, showing no signs of decomposition either visibly or in the IR spectrum. The derivatives HL^1–HL^6 thus behave as tridentate monoanionic ligands on deprotonation. The PNO compounds contain formally 'soft' and 'hard' donor groups within the same backbone. Compounds L^1 and L^2 with their propylene and ethylene bridging chains respectively are flexible enough to be able to bind either in a facial or meridional mode to an octahedrally co-ordinated metal ion.

Conductivity measurements for the iron and cobalt complexes support their characterisation as monomeric, monocationic complexes (1:1 electrolytes) of general type $[ML_2][X]$ (M = Fe or Co, X = PF_6 or BPh_4).

A principal feature of the IR spectra of all the complexes is the band ranging between 1575 and 1622 cm^{-1} which is assigned to ν(C=N). The values observed are at the lower end of the range for ν(C=N) which normally appears between 1575 and 1700 cm^{-1},[4] which is consistent with the weakening of the C=N bond expected on co-ordination. These values represent co-ordination shifts (from the free Schiff base) of approximately 25–30 cm^{-1} lower for the PNO ligands L^1–L^3, about 35–40 cm^{-1} lower for the NNO ligands L^4 and L^5, and virtually no co-ordination shift (0–10 cm^{-1}) for the NNS ligand L^6. The C=N stretching frequency does not appear to be affected by the actual amount of electron density on the metal centre to any great extent, since it seems to be virtually identical for both cationic cobalt and iron complexes and neutral nickel and rhenium complexes. Informative NMR studies of the iron complexes are precluded by their paramagnetism and the insolubility of the nickel complexes prevented any solution measurements. The ^{1}H NMR spectra of the cobalt complexes are also rather uninformative, but they do confirm the diamagnetism, indicating low-spin cobalt(III) (d^6). The ^{31}P NMR spectra of these complexes showed a singlet consistent with the observed structures.

The observed range of room-temperature magnetic moments for the iron complexes in Table 1 of 5.1–5.97 μ_B indicates that

Table 1 Analytical and spectroscopic data

Complex	Colour	Yield (%)	HPLC data[a]	$\tilde{\nu}$(C=N)[b]/cm^{-1}	Analysis (%)[c] C	H	N	μ_{eff}[d]/μ_B
$[FeL^1_2][PF_6]$	Burgundy	62	11.2	1595	58.5 (59.2)	4.3 (4.7)	2.9 (3.1)	5.8
$[FeL^2_2][PF_6]$	Dark green	60	11.4	1605	58.6 (58.3)	4.6 (4.4)	3.1 (3.2)	5.97
$[FeL^3_2][PF_6]$	Green-brown	58	11.5	1622	61.4 (61.2)	6.2 (5.9)	2.7 (2.9)	5.7
$[FeL^4_2][PF_6]$	Green-black	64	10.6	1585	47.9 (48.1)	3.2 (3.0)	9.1 (9.3)	5.6
$[FeL^5_2][PF_6]$	Green-brown	71	10.2	1580	43.0 (43.0)	3.1 (2.7)	8.4 (8.4)	5.1
$[FeL^6_2][PF_6]$	Black	66	9.8	1590	48.0 (47.6)	3.6 (3.4)	8.5 (8.5)	5.4
$[CoL^1_2][PF_6]$	Burgundy	64	10.9	1602	59.4 (58.9)	5.0 (4.7)	3.0 (3.1)	—
$[CoL^2_2][PF_6]$	Dark green	57	11.0	1610	57.4 (58.1)	4.4 (4.4)	3.1 (3.2)	—
$[CoL^3_2][PF_6]$	Burgundy	71	11.2	1600	61.7 (62.2)	4.3 (4.0)	2.4 (2.9)	—
$[CoL^4_2][PF_6]$	Red-black	61	10.2	1580	48.1 (48.2)	3.3 (3.0)	9.1 (9.3)	—
$[CoL^5_2][PF_6]$	Red	81	10.2	1575	43.4 (43.1)	3.0 (2.7)	8.6 (8.4)	—
$[CoL^6_2][PF_6]$	Dark brown	65	10.4	1590	47.7 (47.4)	3.5 (3.3)	8.7 (8.5)	—
$[NiL^1_2]$	Yellow	48	8.6	1620	69.7 (70.3)	5.7 (5.6)	3.5 (3.7)	2.9
$[NiL^2_2]$	Orange	53	8.8	1602	70.1 (69.7)	5.4 (5.3)	3.7 (3.9)	3.2
$[NiL^4_2]$	Orange	83	8.3	1580	63.9 (63.6)	4.5 (4.4)	12.3 (12.4)	3.0
$[NiL^5_2]$	Green	88	8.4	1600	55.4 (55.2)	3.2 (3.1)	10.5 (10.7)	3.1
$[NiL^6_2]$	Green	86	8.2	1580	61.3 (61.9)	4.8 (4.7)	10.7 (10.9)	3.2
$[ReOCl_2L^2]$	Olive green	32	10.9	1620	41.8 (41.6)	3.3 (3.1)	2.2 (2.3)	—
$[ReOCl_2L^3]$	Dark orange	34	11.0	1590	46.1 (45.9)	3.3 (2.9)	2.0 (2.1)	—

[a] In thf–water in the presence of $[NBu^n_4][BF_4]$. [b] As Nujol mulls, KBr plates. [c] Calculated values in parentheses. [d] Measured at room temperature.

the iron(III) nucleus is essentially high spin (spin-only value 5.9 μ_B).[5] The magnetic behaviour is complicated by spin crossover, and this is discussed in more detail below. The observed magnetic moments for the nickel complexes of 2.9–3.2 μ_B are in the expected range for high-spin octahedral Ni^{II} with two unpaired electrons.[5]

Electrochemical Measurements.—The complexes of Fe^{III} and Co^{III} reported above all showed completely irreversible electrochemical behaviour and will not be discussed further. The redox characteristics of the complexes of the type $[ReOCl_2L]$ (L = L^1–L^3) have been studied in some detail.

Complexes with L^1 *and* L^3. The cyclic voltammogram of $[ReOCl_2L^3]$ in dichloromethane at room temperature is shown in Figure 1(*i*). The full details of the electrochemical processes are summarised in Table 2. The oxidative (A) and reductive (B) processes are both completely irreversible at room temperature. The addition of $[NBu^n_4]Cl$ as support electrolyte caused no improvement in the electrochemical reversibility of B, indicating that chloride loss is not responsible for the irreversibility. At 200 K [Fig. 1(*ii*)] the reduction process is quasi-reversible at a scan rate of 0.2 V s^{-1}, but becomes fully Nernstian at a 5 V s^{-1} scan rate.

The complex $[ReOCl_2L^1]$ at room temperature [Fig. 2(*i*)] shows a quasi-reversible oxidation (C) at $E_{\frac{1}{2}}$ +1.00 V and a reduction (D) at −1.20 V. The latter potential indicates that the complex is some 200 mV easier to reduce than that with L^3. The oxidation process is very similar for both complexes showing that the energy of the highest occupied molecular orbital (HOMO) is independent of the ligand. Both processes become essentially Nernstian at 200 K [Fig. 2(*ii*)]. All redox potentials in Table 2 are quoted relative to the ferrocene–ferrocenium couple as internal standard, taken as 0.0 V, whereas the potential axes in Figs. 1–3 are relative to an AG pseudo-reference electrode.

Complex with L^2. The redox behaviour of $[ReOCl_2L^2]$ is more complex, the cyclic voltammogram in dichloromethane at room temperature showing clear evidence for the presence of two species in solution. These exhibit quasi-reversible oxidation (E_1 and E_2) and reduction steps (F_1 and F_2), broadly similar as expected to those for the L^1 complex [Fig. 3(*i*)]. There are also some processes attributable to the redox-active species generated by the chemical steps following electron transfer. As previously all four principal processes become Nernstian at 200 K [Fig. 3(*ii*)]. The ^{31}P NMR spectrum of the complex (see Experimental section) shows two singlets and we provisionally identify these as the isomers with *mer* and *fac* ligation of the ligand. The crystal structure of the complex with L^1 confirmed a *fac* configuration[2] and it appears that the shorter ethylene backbone of the L^2 ligand favours the formation of some of the *mer* isomer. However in the absence of additional information we cannot entirely rule out the possibility of alternative isomers such as those with the oxo-group *trans* to the imine nitrogen.

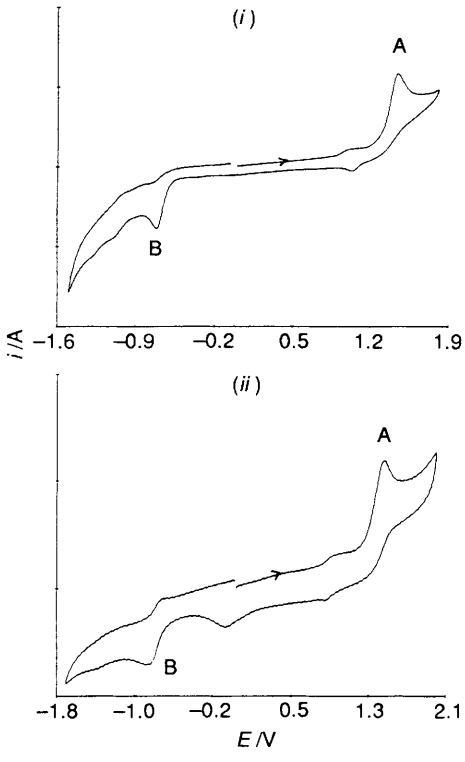

Fig. 1 Cyclic voltammogram for $[ReOCl_2L^3]$ in CH_2Cl_2 at 293 (*i*) and 200 K (*ii*) at scan rates of 0.2 V s^{-1}

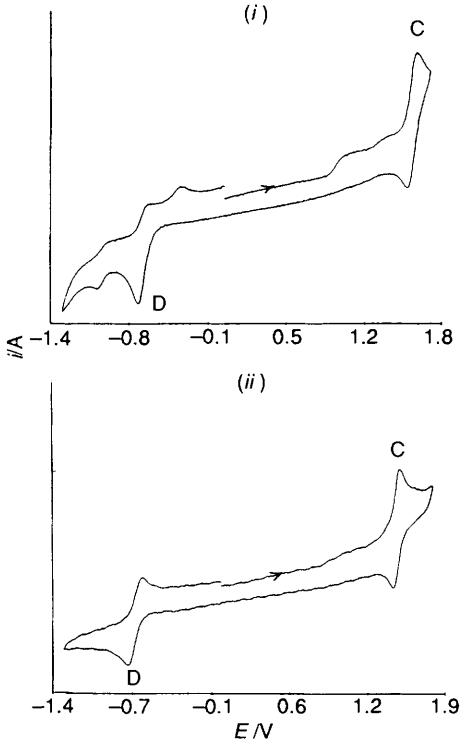

Fig. 2 Cyclic voltammogram for $[ReOCl_2L^1]$ in CH_2Cl_2 at 293 (*i*) and 200 K (*ii*) at scan rates of 0.2 V s^{-1}

Mössbauer Measurements.—Iron(III) octahedral complexes exhibit a temperature-dependent spin crossover if the ligand-field strength is comparable to the mean spin-pairing energy. The spin-crossover event involves an intramolecular transfer of two electrons from the e_g to t_{2g} orbitals. Much work has been done in studying the kinetics and mechanism of spin-crossover transformations.[6–8] The spin-state interconversion rate has been shown to be sensitive to the counter ion and ligand substituents.[9] The exact origins of these effects are at present undetermined. A review of the literature shows few examples of spin interconversion in complexes containing tridentate ligands; the majority of the work has been done using bi-, penta- and hexa-dentate ligands.

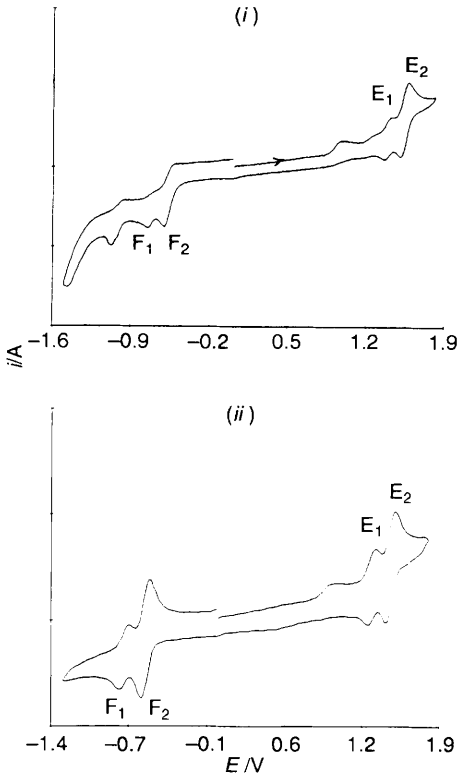

Fig. 3 Cyclic voltammogram for $[ReOCl_2L^2]$ in CH_2Cl_2 at 293 (*i*) and 200 K (*ii*) at scan rates of 0.2 V s^{-1}

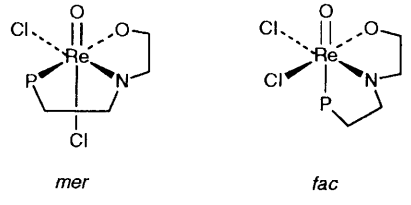

The temperature dependence of the Mössbauer spectra of the $[FeL^1{}_2]^+$ and $[FeL^3{}_2]^+$ cations with both PF_6^- and BPh_4^- are shown in Figs 4 and 5. The data are also summarised in Table 3.

$[FeL^1{}_2]^+$. Both the PF_6 and BPh_4 salts show evidence for both high- and low-spin sites at all the temperatures investigated. The relative proportion of the two sites is strongly anion dependent, with 45% of low spin for the PF_6 salt compared with 75% for the BPh_4 salt at 78 K. It is also apparent that the metal environment for the high-spin site is different for the two anions. There is an obvious quadrupole splitting for the PF_6 salt (zero for the BPh_4 salt), and the isomer shift is much larger. By contrast the isomer shift values for the low-spin sites are similar for the two anions. The fact that the changes in spin state occur over such a large temperature range suggests that the spin-crossover equilibria involved are second order.

$[FeL^3{}_2]^+$. The situation here is dramatically different, with the PF_6 salt only showing a single high-spin site at both 78 and 293 K. However, the BPh_4 salt again shows spin-crossover behaviour, but with only 25% of the low-spin site present at 78 K. Again there is a difference in the quadrupole splitting of the high-spin sites with the two anions.

Table 2 Electrochemistry of the complexes $[ReOCl_2L]$ (L = L^1–L^3)*

Ligand	$E_{\frac{1}{2}}$/V	i_{pa}/i_{pc}	E_p/mV	T/K
Oxidation processes				
L^1	0.94	1.27	88	200
	1.00	1.62	104	293
L^2	0.96	1.07	61	200
	0.81	0.96	47	200
	1.01	1.04	72	293
	0.87	1.09	64	293
L^3	E_{pa} = 0.96	> 1	—	200
	E_{pa} = 0.92	> 1	—	293
Reduction processes				
L^1	−1.27	0.77	135	200
	−1.20	0.41	78	293
	−1.52	—	85	293
L^2	−1.12	0.94	61	200
	−1.30	1.07	74	200
	−1.09	0.40	79	293
	−1.52	0.37	85	293
L^3	−1.33	0.5	144	200
	E_{pc} = −1.24	> 1	—	293
	E_{pc} = −1.61	—	—	293
	E_{pc} = −1.82	—	—	293

* All potentials quoted relative to ferrocene–ferrocenium as 0.0 V (added as internal standard).

Table 3 Mössbauer data (mm s^{-1})

Compound	T/K	δ	Δ	$\Gamma_{\frac{1}{2}}$	Total site (±3%)
$[FeL^1_2][PF_6]$	78	0.32(1)	2.11(1)	0.19(1)	45
		0.55(1)	0.82(1)	0.31(1)	55
	293	0.17(1)	2.06(1)	0.15(1)	24
		0.36(1)	0.75(1)	0.28(1)	76
$[FeL^3_2][PF_6]$	78	0.45(1)	0.72(1)	0.24(1)	100
	293	0.41(1)	0.70(1)	0.23(1)	100
$[FeL^1_2][BPh_4]$	78	0.26(1)	2.16(1)	0.50(1)	75
		0.30(1)	—	0.36(1)	25
	150	0.25(1)	2.17(1)	0.44(1)	59
		0.31(1)	—	0.39(1)	41
	200	0.17(1)	2.34(1)	0.35(1)	50
		0.29(1)	—	0.36(1)	50
	293	0.12(1)	2.22(1)	0.29(1)	39
		0.18(1)	—	0.38(1)	61
$[FeL^3_2][BPh_4]$	78	0.36(1)	1.33(1)	0.20(1)	25
		0.29(1)	0.29(1)	0.19(1)	75
	50	0.36(1)	1.34(1)	0.17(1)	18
		0.26(1)	0.30(1)	0.19(1)	82
	293	0.24(1)	0.28(1)	0.13(1)	100

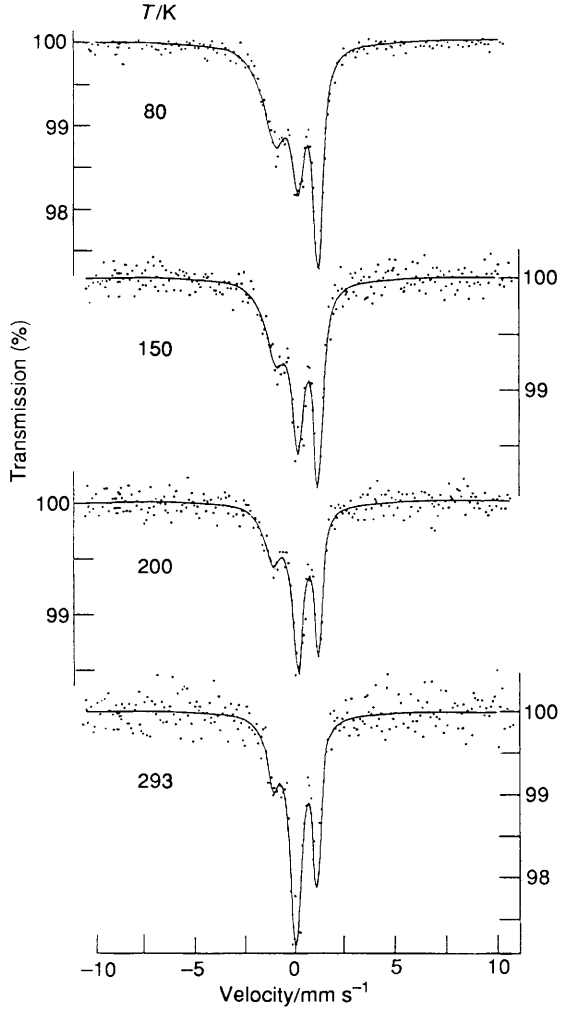

Fig. 4 Temperature dependence of the Mössbauer spectrum of $[FeL^1_2]^+$

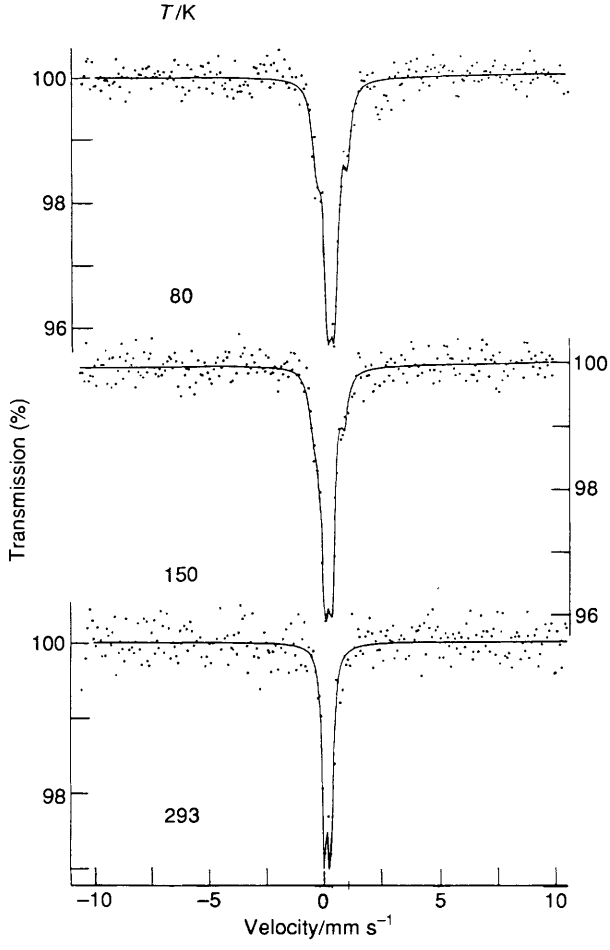

Fig. 5 Temperature dependence of the Mössbauer spectrum of $[FeL^3_2]^+$

The strong anion dependence of the spin-crossover phenomenon is well documented, and presumably reflects the variations in solid-state packing effects caused by the different packing requirements of the two anions. It appears that the more flexible ligand L^1 is more readily distorted by the packing effects which trigger the spin-state change. It seems unlikely that there is any

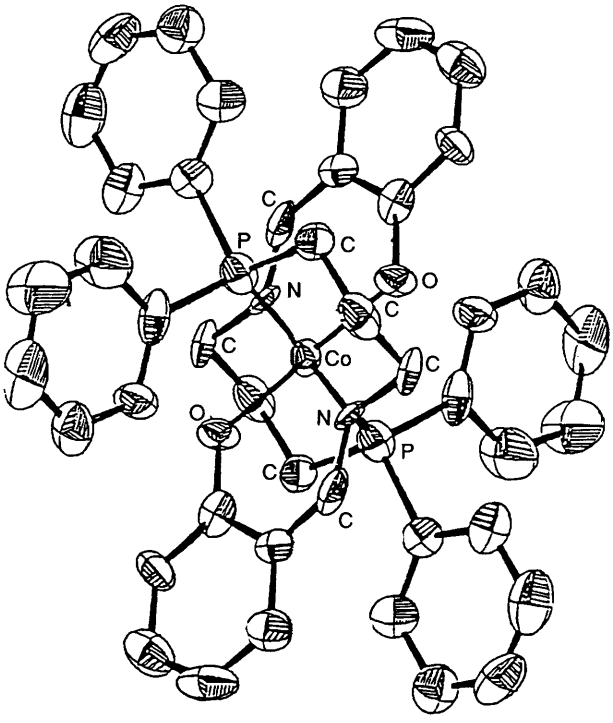

Fig. 6 An ORTEP[10] plot of the structure of $[CoL^1_2]^+$

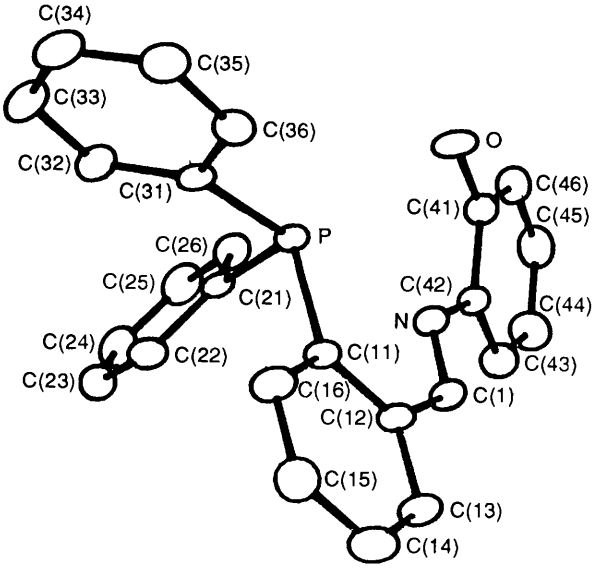

Fig. 7 An ORTEP plot of the structure of HL^3

radical change in geometry from say *fac-fac* to *mer-mer* co-ordination, as the energies available are small, and the two sites are readily interconvertible. It therefore seems probable that the packing effects cause small changes in geometry (as seen from the quadrupole splittings) and that these are more easily accommodated by L^1 with its more flexible backbone. Only the larger BPh_4 anion is able to induce the distortions necessary to cause the spin-state change with the more rigid L^3 ligand. We are currently investigating the Mössbauer spectra of these complexes in more detail, but regrettably attempts to grow crystals with different anions suitable for an X-ray diffraction study have been unsuccessful to date.

Crystal Structure of $[CoL^1_2][BPh_4]$.—A crystal structure determination was carried out on $[CoL^1_2]^+$, but unfortunately the crystal quality was not good, and the final R value did not fall below 0.126. Consequently we restrict ourselves to a graphical representation of the structure (Fig. 6) and a brief discussion.

Table 4 Positional parameters for $2\text{-}Ph_2PC_6H_4CH{=}NC_6H_4OH$ (HL^3)

Atom	x	y	z
P	0.516 54(2)	0.189 61(5)	0.632 34(2)
O	0.588 03(8)	0.403 2(2)	0.747 82(7)
N	0.607 35(7)	0.099 5(2)	0.724 92(6)
C(1)	0.590 70(9)	−0.044 6(2)	0.724 98(8)
C(11)	0.500 22(8)	−0.023 7(2)	0.639 02(7)
C(12)	0.538 25(9)	−0.111 9(2)	0.682 42(8)
C(13)	0.525 0(1)	−0.273 4(2)	0.685 81(9)
C(14)	0.475 3(1)	−0.348 1(2)	0.648 6(1)
C(15)	0.438 2(1)	−0.262 3(3)	0.607 0(1)
C(16)	0.450 6(1)	−0.102 8(2)	0.602 09(9)
C(21)	0.599 22(9)	0.183 4(2)	0.602 84(8)
C(22)	0.610 25(9)	0.077 2(2)	0.561 47(8)
C(23)	0.673 0(1)	0.075 5(3)	0.540 16(9)
C(24)	0.726 4(1)	0.178 1(3)	0.560 76(9)
C(25)	0.716 5(1)	0.283 0(3)	0.601 1(1)
C(26)	0.652 9(1)	0.286 6(2)	0.622 10(9)
C(31)	0.452 09(9)	0.245 5(2)	0.572 40(7)
C(32)	0.468 46(9)	0.295 9(2)	0.522 24(8)
C(33)	0.417 0(1)	0.357 3(3)	0.482 66(9)
C(34)	0.348 5(1)	0.369 5(3)	0.492 5(1)
C(35)	0.331 1(1)	0.319 0(3)	0.542 0(1)
C(36)	0.382 24(9)	0.259 3(3)	0.581 93(8)
C(41)	0.646 9(1)	0.330 5(2)	0.773 15(8)
C(42)	0.658 24(9)	0.170 3(2)	0.764 25(7)
C(43)	0.718 8(1)	0.099 6(3)	0.790 88(9)
C(44)	0.767 7(1)	0.185 8(3)	0.825 3(1)
C(45)	0.756 2(1)	0.343 7(3)	0.833 67(9)
C(46)	0.695 8(1)	0.415 2(2)	0.808 39(9)

The overall structure has two independent molecules sitting at centres of symmetry with the tetraphenylborate groups situated between them. There appear to be no significant differences between equivalent bond distances in the two molecules. Each Co is essentially octahedrally co-ordinated by 2P, 2O and 2N atoms, each pair being mutually *trans*. At first sight the adoption of the facial mode of co-ordination for the ligands is surprising in view of the presence of the flexible trimethylene backbone, but this does permit the bulky PPh_2 groups to be as far apart as possible, and a similar configuration is seen for the complex $[ReOCl_2L^1]$.[2]

Crystal Structure Determinations of HL^3 *and* $[CoL^3_2][PF_6]$.—The molecular structure and atom labelling scheme for HL^3 is shown in Fig. 7. Fractional atomic coordinates appear in Table 4, selected bond lengths, angles and torsion angles in Table 5. Details of the structure determination are summarised in Table 7. The structure of the complex cation $[CoL^3_2]^+$ is shown in Fig. 8, together with an atom labelling scheme. Fractional atomic coordinates are presented in Table 6 and selected bond lengths and angles in Table 5 for comparison. In the discussion below the numbering scheme for HL^3 is used unless otherwise indicated.

In both HL^3 and $[CoL^3_2]^+$ the C(12)–C(1)=N–C(42) imino-units are *trans* planar. Internal bond lengths and angles in the free and co-ordinated Schiff bases are similar, although there is some lengthening of the C(1)=N bonds in the metal complex.

The configuration of HL^3 is somewhat surprising in that the P atom approaches N and O(1) rather than swinging away by rotation about the C(1)–C(12) bond. It is not clear exactly why this should occur, but it does preorganise L^3 in an ideal way to co-ordinate to the metal in a facial geometry (see below). The atoms C(31), P, C(11)–C(16), C(1), N, and C(42) are coplanar (maximum deviation 0.032 Å for P), but the iminophenol ring twists 30.6° out of this plane [as measured by the mean of the torsion angles about N–C(42)]. This torsion, together with

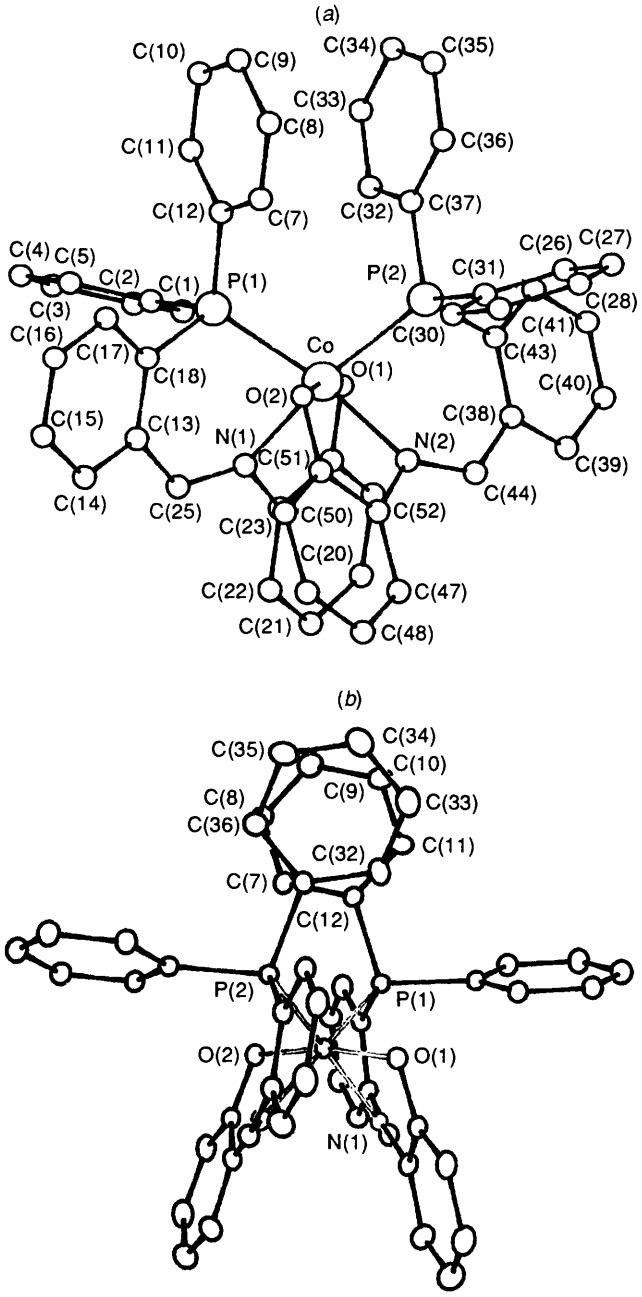

Fig. 8 (*a*) A PLUTO[11] plot of the structure of $[CoL^3{}_2]^+$, showing the labelling scheme. (*b*) An ORTEP plot of the structure showing the stacking of phenyl rings

some opening of the angles at C(1), N and C(42) above 120°, almost certainly reduces steric interaction of H(1) and H(43), as occurs for benzylideneanilines[3,15–18] and in *N*-phenyl Schiff bases of ferrocenecarbaldehyde.[19] Analysis of the C(11)–C(21)–C(31) plane shows that the lone pair of electrons on P lies on the same side of the *trans* imino unit as does O(1).

In the complex cation $[CoL^3{}_2]^+$ the metal is bonded in a pseudo-octahedral geometry by two L^3 ligands, both arranged in *fac* configurations. The O atoms are *trans* to one another, the nitrogen atoms *cis* and the P atoms *cis*. An approximate two-fold axis bisects the P(1)–Co–P(2) and N(1)–Co–N(2) angles, as shown in Fig. 8. The structures of the two ligands are very similar. The P · · · O distance in HL^3 (3.48 Å) is much too short to allow L^3 to bind at the metal in a *mer* cofiguration. This is shown by comparison of the sum of the Co–O and Co–P distances in $[CoL^3{}_2]^+$ where both sums are 4.16 Å, and P and O(1) could not adopt *trans* co-ordination sites.

The conformations of the ligands are modified as compared with free HL^3, but the changes may be described by a sequence of minimum movements. First the iminophenyl ring is brought into coplanarity with the imino-unit by torsion of about 30° about the N–C(42) bond. Secondly the imino-unit is swivelled about its terminating bonds, N–C(42) and C(1)–C(12), by about 25°, bringing the nitrogen lone pair out of the plane of the phenyl rings. There is a third small adjustment of the phosphorus lone pair by rotation about the P–C(11) bond. The P–C(11)–C(16) and iminophenyl planes in each ligand are within 10° of being parallel (but not coplanar). In each ligand the P and O atoms lie on the same side of the imino-plane with the cobalt atom lying on the opposite side.

The relative dispositions of the PPh rings C(7)–C(12) and C(32)–C(37) (complex numbering scheme) form an interesting feature of the structure of the complex. They are almost parallel, 3.4 Å apart, and are in a staggered configuration. Fig. 8(*b*) shows the overlay of the two rings.

Experimental

All air-sensitive manipulations were carried out under an atmosphere of dry dinitrogen. Standard Schlenk-tube, vacuum-line and syringe techniques were utilised throughout where appropriate. Melting points were determined using an electrothermal apparatus. Elemental analyses were performed by Medac, University of Brunel. Electron-impact mass spectra were recorded by the SERC Mass Spectrometry Service Centre, University College Swansea, using 3-nitrobenzyl alcohol as the matrix, infrared spectra in the range 200–4000 cm^{-1} as Nujol mulls (KBr plates) on a Perkin-Elmer spectrophotometer 1331 and ^1H, ^{13}C and ^{13}P NMR spectra using a Bruker WP80SY spectrometer. Conductivity measurements were performed using a Jenway meter. Room-temperature magnetic moments were determined using a Johnson Matthey magnetic susceptibility balance. Mössbauer spectra were recorded using the experimental procedures described previously.[20] Solvents were dried by standard methods[21] and redistilled before use. (3-Aminopropyl)diphenylphosphine was prepared from diphenylphosphine and allylamine according to previously described procedures.[22] (2-Aminoethyl)diphenylphosphine was prepared from diphenylphosphinolithium and ethyleneimine.[23] 2-(Diphenylphosphino)benzaldehyde was prepared according to the literature procedure.[24] All other reagents were used as received.

Preparation of the Schiff Bases.—2-$[Ph_2P(CH_2)_3N{=}CH]C_6H_4OH$, HL^1. Salicylaldehyde (3.66 g, 0.03 mol) in ethanol (5 cm^3) was added to a solution of freshly prepared (3-aminopropyl)diphenylphosphine (30 mmol) in ethanol–thf (30 cm^3).[22] The solution was then heated to reflux for 2 h, during which time the yellow colour of the final product develops. The volume was then reduced under vacuum to *ca.* 15 cm^3, and the flask placed in a deep freeze for 6 h. The yellow microcrystalline solid that precipitated was filtered off at the pump, washed with cold ether–methanol and dried under vacuum. Yield 7.6 g (73%). NMR ($CDCl_3$): ^1H (80 MHz), δ 13.5 (1 H, br, OH), 8.3 (1 H, s, CH=N), 7.7–6.7 (m, aromatic H), 3.6 (t, $^3J_{HH}$ = 6.4 Hz, NCH_2) and 2.4–1.7 (m, PCH_2); ^{13}C (32 MHz), δ 165.1 (s, COH), 161.2 (s, CH=N), 138.7–116.9 (m, aromatic C), 59 (d, J_{CN} = 13.4, NCH_2) and 26.5 (dd, J_{CF} = 12 Hz, PCH_2); ^{31}P (32 MHz), δ −15.7 (1 P, s, Ph_2P) (Found: C, 74.1; H, 7.2; N, 4.4. $C_{22}H_{22}NOP$ requires C, 74.3; H, 7.4; N, 4.1%); ν(OH) 1275s, 1150m; ν(C=N) 1625m cm^{-1}; HPLC retention time = 9.0 min; *m/z* 347 (M^+).

2-$[Ph_2P(CH_2)_2N{=}CH]C_6H_4OH$, HL^2. Salicylaldehyde (3.66 g, 0.03 mol) in ethanol (5 cm^3) was added to a solution of freshly prepared (2-aminoethyl)diphenylphosphine (30 mmol) in ethanol–thf (30 cm^3).[23] The solution was then heated to reflux for 1 h, during which time the final yellow colour of the product develops. On cooling in the deep freeze for 6 h a pale yellow solid separated. This was filtered off at the pump, and washed with cold methanol–ether. The filtrate afforded more

Table 5 Selected bond lengths (Å), bond and torsion angles (°) for $[CoL^3_2]^+$ with values for HL^3 in square brackets

	$[CoL^3_2]^+$		$[CoL^3_2]^+$
Co–P(1)	2.234(4)	Co–N(1)	1.975(6)
Co–P(2)	2.240(4)	Co–N(2)	1.980(8)
Co–O(1)	1.923(6)	C(25)=N(1)	1.249(9) [1.269(3)]
Co–O(1)	1.917(6)	C(44)=N(2)	1.295(10)
P(1)–Co–N(1)	83.5(3)	O(1)–Co–O(2)	170.3(2)
P(1)–Co–P(2)	104.7(2)	N(1)–Co–N(2)	90.7(3)
O(2)–Co–P(2)	100.7(2)	C(13)–C(25)–N(1)	122.6(7) [121.8(2)]
P(2)–Co–N(2)	83.5(3)	C(38)–C(44)–N(2)	123.1(7)
P(2)–Co–N(1)	166.7(2)	C(25)–N(1)–C(23)	122.0(7) [124.4(2)]
P(1)–Co–N(2)	166.4(2)	C(44)–N(2)–C(52)	122.0(7)
N–C(1)–C(12)–C(11)	24(1), 25(1) [2.1(3)]		
N–C(1)–C(12)–C(13)	−157.0(7), 157.1(7) [−178.6(2)]		
C(1)–N–C(42)–C(41)	156.4(6), 158.3(6) [151.7(2)]		
C(1)–N–C(42)–C(43)	−27(1), −24(1) [−33.0(3)]		
C(12)–C(11)–P–C(21)	77.5(6), 79.0(6) [77.2(2)]		
C(12)–C(11)–P–C(31)	−172.4(5), −170.9(5) [−177.8(1)]		

The numbering scheme for HL^3 is used except when the Co is involved and the scheme for the complex is then utilised.

Table 6 Positional parameters for $[CoL^3_2][PF_6]$

Atom	*x*	*y*	*z*	Atom	*x*	*y*	*z*
Co	2479(1)	1624(1)	71(1)	C(27)	1065(2)	605(3)	−3111(2)
P(1)	2374(1)	851(1)	1097(1)	C(28)	197(2)	748(3)	−2913(2)
O(1)	3756(3)	1716(3)	78(3)	C(29)	44(2)	940(3)	−2130(2)
N(1)	2646(3)	2375(3)	924(3)	C(30)	757(2)	990(3)	−1546(2)
C(1)	4187(3)	919(3)	1690(2)	C(31)	1625(2)	848(3)	−1744(2)
C(2)	4885(3)	840(3)	2286(2)	C(32)	3714(3)	−194(3)	−336(3)
C(3)	4707(3)	616(3)	3053(2)	C(33)	4044(3)	−911(3)	−240(3)
C(4)	3830(3)	471(3)	3224(2)	C(34)	3617(3)	−1491(3)	−664(3)
C(5)	3132(3)	550(3)	2628(2)	C(35)	2862(3)	−1355(3)	−1183(3)
C(6)	3310(3)	774(3)	1861(2)	C(36)	2533(3)	−637(3)	−1279(3)
C(7)	1252(3)	−216(2)	374(3)	C(37)	2959(3)	−57(3)	−856(3)
C(8)	980(3)	−938(2)	197(3)	C(38)	3450(5)	2094(4)	−1636(4)
C(9)	1466(3)	−1531(2)	537(3)	C(39)	4098(5)	2436(5)	−2060(4)
C(10)	2226(3)	−1402(2)	1055(3)	C(40)	4776(6)	2009(5)	−2351(5)
C(11)	2498(3)	−681(2)	1233(3)	C(41)	4794(5)	1267(5)	−2237(5)
C(12)	2012(3)	−88(2)	892(3)	C(42)	4130(5)	905(4)	−1835(4)
C(13)	1516(4)	2030(4)	1807(4)	C(43)	3455(5)	1320(4)	−1526(4)
C(14)	882(5)	2342(4)	2252(4)	C(47)	1420(5)	3579(4)	−719(4)
C(15)	195(5)	1911(5)	2531(5)	C(48)	649(6)	3913(5)	−453(4)
C(16)	157(5)	1173(5)	2355(5)	C(49)	61(6)	3494(5)	−21(5)
C(17)	812(5)	837(5)	1919(4)	C(50)	234(5)	2760(5)	175(4)
C(18)	1487(4)	1267(4)	1643(4)	C(51)	996(4)	2416(4)	−89(4)
C(19)	4711(5)	2783(5)	−6(4)	C(52)	1570(4)	2843(4)	−542(4)
C(20)	4853(5)	3522(5)	188(5)	C(44)	2764(5)	2576(4)	−1347(4)
C(21)	4250(6)	3917(5)	629(5)	P(3)	7380(2)	1174(2)	3864(2)
C(22)	3501(5)	3561(4)	892(4)	F(1)	8059(5)	611(5)	4303(5)
C(23)	3378(4)	2818(4)	717(4)	F(2)	6965(5)	582(5)	3270(5)
C(24)	3959(4)	2419(4)	265(4)	F(3)	6713(5)	928(6)	4466(6)
C(25)	2204(5)	2523(4)	1535(4)	F(4)	7763(6)	1752(5)	4483(6)
P(2)	2579(1)	888(1)	−992(1)	F(5)	6692(7)	1719(5)	3493(7)
O(2)	1208(3)	1711(3)	77(2)	F(6)	8062(7)	1374(9)	3297(6)
N(2)	2308(4)	2407(3)	−751(3)	C(45)	7989(9)	4385(8)	1127(8)
C(26)	1779(2)	655(3)	−2526(2)	C(46)	7706(12)	3722(11)	1402(10)

solid on reduction of the volume under vacuum to *ca.* 10 cm^3, followed by cooling in the deep freeze for 6 h. Yield 6.3 g (63%), NMR ($CDCl_3$): ^1H (80 MHz), δ 8.4 (1 H, s, CH=N), 7.7–6.8 (m, 14 H, aromatic H), 4.2–3.6 (m, 2 H, NCH_2) and 2.8–2.5 (m, 2 H, PCH_2); ^{13}C (20 MHz), δ 164.9 (s, N=CH), 161.4 (s, COH), 56.5 (d, J_{CN} = 21, CH_2N) and 29.8 (d, J_{CP} = 13.1 Hz, CH_2P); ^{31}P (32 MHz), δ −18.6 (1 P, s, Ph_2P) (Found: C, 75.9; H, 6.1; N, 4.2. $C_{21}H_{20}NOP$ requires C, 75.6; H, 6.2; N, 4.0%); ν(OH) 3400 (br), 1282m, 1155m, ν(C=N) 1630s cm^{-1}; HPLC retention time = 9.2 min; *m/z* 333 (M^+).

2-(2-$Ph_2PC_6H_4CH$=N)C_6H_4OH, HL^3. Aminophenol (1.53 g, 14 mmol) in ethanol (10 cm^3) was added dropwise to 2-(diphenylphosphino)benzaldehyde (4 g, 14 mmol) in ethanol (20 cm^3). The solution was then heated under reflux for 2 h, during which time the yellow colour of the product develops. After cooling the mixture was evaporated to *ca.* 15 cm^3, and placed in a freezer. A yellow microcrystalline solid precipitated over 6 h. This was filtered off, washed with cold methanol–ether and dried *in vacuo*. Yield 4.2 g (78%). NMR ($CDCl_3$): ^1H (80 MHz), δ 9.03 (1 H, d, J_{PH} = 5.5, CH=N) and 8.0–6.5 (18 H, m, aromatic H); ^{13}C (32 MHz), δ 156.5 (d, J_{CP} = 12 Hz, CH=N), 152.2 (s, COH) and 139.3–128.5 (m, aromatic C); ^{31}P (32 MHz), δ −9 (1 P, s, PhP) (Found: C, 79.2; H, 5.4; N, 3.5. $C_{25}H_{20}NOP$ requires C, 78.9; H, 5.3; N, 3.6%); ν(OH) 3275 (br), 1250s, 1125w; ν(C=N) 1625m cm^{-1}; HPLC retention time = 9.4 min; *m/z* 381 (M^+).

Table 7 Summary of crystal data, data collection and structure refinement for HL^3 and $[CoL^3{}_2][PF_6]$[a]

	$[CoL^3{}_2][PF_6]$	HL^3
Empirical formula	$[C_{52}H_{38}CoF_6N_2O_2P_3]$[b]	$C_{25}H_{20}NOP$
Colour, habit	Deep red prisms	Yellow needles
M	988.73	381.42
Space group	$P2_1/c$	$C2/c$
a/Å	15.01(2)	19.174(10)
b/Å	18.12(3)	8.527(2)
c/Å	16.76(1)	24.563(12)
β/°	94.73(1)	98.22(2)
U/Å^3	4548.7	3975(5)
Z	4	8
D_c/g cm^{-3}	1.44	1.27
μ/cm^{-1}	5.46	1.5
Crystal dimensions/mm	0.3 × 0.22 × 0.15	0.4 × 0.5 × 0.6
F(000)	2024	1600
Diffractometer	Enraf-Nonius FAST	Enraf-Nonius CAD4
2θ range/°	1.5–52	0–50
Scan speed/° min^{-1}	—	1–7 (in ω)
Reflections collected	26 004, 10 535 unique	4122
Reflections used	4516 ($F_o > 5\sigma F_o$)	2913 ($F_o > 3\sigma F_o$)
Absorption correction	DIFABS[12]	Empirical
System used	SHELX 80[13]	MOLEN[14]
Solution	Patterson	Direct methods
Hydrogen atoms	Not included	Not refined, included in structure factors
Weighting scheme	Unit weights	$w = [\sigma^2(F_o) + 0.0004F_o^2]^{-1}$
R, R'	0.058, 0.069	0.044, 0.065

[a] Details in common: monoclinic; Mo-Kα radiation (λ 0.710 69 Å); 291 K; graphite-crystal incident-beam monochromator; full-matrix least-squares refinement. [b] The lattice also contains some disordered methanol of solvation which was modelled as two carbon atoms since identification of C and O was not unequivocal; these atoms are included in the formula.

2-[2-(C_5H_4N)CH=N]C_6H_4OH, HL^4. Pyridine-2-carbaldehyde (5 g, 0.05 mol) and 2-aminophenol (5.1 g, 0.05 mol) in ethanol (15 cm^3) were heated under reflux for 1 h, during which time the pale yellow colour of the final product develops. The solvent was then removed under vacuum to yield a yellow oil which was recrystallised from hot ethanol. The yellow crystals were then filtered off at the pump, and washed with cold methanol–ether. Yield 8.7 g (87%), m.p. 109 °C (lit.,[1] 108 °C) (Found: C, 73.6; H, 3.1; N, 14.4. $C_{12}H_{10}N_2O$ requires C, 72.7; H, 3.1; N, 14.1%); ν(C=N) 1622m (lit.,[1] 1627); ν(OH) 3360 (br), 1285m, 1155s cm^{-1}; HPLC retention time = 7.6 min; m/z 198 (M^+) and 181 (M − OH). NMR ($CDCl_3$): ^{1}H (60 MHz), δ 8.1 (1 H, s, CH=N), 7.2–8.1 (7 H, m, aromatic protons) and 8.3 (1 H, d, J_{HH} = 2.3 Hz, o-pyridyl proton); ^{13}C (20 MHz), δ 157.14 (s, CH=N) and 136.6 (s, COH). λ_{max}(dmf) 359 and 292 nm.

2-[2-(C_5H_4N)CH=N]-4-Cl-C_6H_3OH, HL^5. Compound HL^5 was similarly prepared from pyridine-2-carbaldehyde (5 g, 0.05 mol) and 5-chloro-2-hydroxyaniline (7.3 g, 0.05 mol) in ethanol (30 cm^3) under reflux for 2 h to yield pale orange crystals upon cooling. Yield 9.8 g (84%), m.p. 142 °C (Found: C, 61.7; H, 3.8; N, 12.3. $C_{12}H_9ClN_2O$ requires C, 62.0; H, 3.9; N, 12.0%); ν(C=N) 1620w; ν(OH) 3880w, 1280m, 1170w cm^{-1}; HPLC retention time = 9.6 min; m/z 233 (M^+) and 216 (M − OH). NMR ($CDCl_3$): ^{1}H (60 MHz), δ 8.0 (1 H, s, CH=N), 6.8–8.2 (6 H, m, aromatic protons) and 8.5 (1 H, m, o-pyridyl proton); ^{13}C (20 MHz), δ 158.0 (s, CH=N), 136.8 (s, COH) and 116.6 (s, CCl). λ_{max}(dmf) 365 and 290 nm.

2-[2-(C_5H_4N)CMe=N]C_6H_4SH, HL^6. Compound HL^6 was prepared from 2-acetylpyridine (5 g, 0.05 mol) and 2-aminobenzenethiol (5.2 g, 0.05 mol) in ethanol (30 cm^3) heated under reflux for 2 h during which time the yellow colour of the final product developed. The solvent was then removed under vacuum to yield a yellow oil which was recrystallised from hot ethanol. The yellow crystals were filtered off at the pump and washed with cold methanol–ether. Yield 7.5 g (81%), m.p. 111 °C (Found: C, 67.1; H, 5.3; N, 12.25. $C_{13}H_{12}N_2S$ requires C, 68.4; H, 5.3; N, 12.3%); ν(C=N) 1590m; ν(SH) 3150 (br) cm^{-1}; HPLC retention time = 11.2 min; m/z 228 (M^+), 213 (M − Me), 196 (M − S) and 195 (M − SH). NMR ($CDCl_3$): ^{1}H (60 MHz) δ 2.25 (3 H, m, CH_3), 6.3–7.0 (7 H, m, aromatic protons) and 8.5 (1 H, d, J_{HH} = 2.04 Hz, o-pyridyl proton); ^{13}C (20 MHz), δ 163.6 (s, CH=N) and 111.9 (s, CSH). λ_{max}(dmf) 345 and 290 nm.

2-$Ph_2PC_6H_4\overline{CHNHC_6H_4S}$, HL^7. 2-(Diphenylphosphino)-benzaldehyde (5 g, 0.02 mol) and 2-aminobenzenethiol (2.16 g, 0.02 mol) in ethanol (30 cm^3) were heated under reflux for 2 h. After reducing the volume under vacuum to *ca.* 15 cm^3, the solution afforded white crystals on cooling. These were filtered off at the pump, washed with cold methanol–ether, and dried under vacuum. Yield 6.3 g (79%) (Found: C, 75.9; H, 5.1; N, 3.2. $C_{25}H_{20}NPS$ requires C, 75.5; H, 5.0; N, 3.5%); m/z 397 (M^+). NMR ($CDCl_3$): ^{1}H (80 MHz), δ 8.5–8.1 (1 H, m, NH), 7.8–6.4 (18 H, m, Ph), 2–1.5 (1 H, br, CH); ^{13}C (20 MHz), δ 66.9 (d, J_{CH} = 6.2 Hz, CH), 120–145 (m, phenyl C) and 147.7 (s, CNH); ^{31}P (32 MHz), δ 34 (s, Ph_2P). HPLC retention time = 11.6 min; ν(N–H) 3180w, 1175m, 720s; ν(C–N) 1175s cm^{-1}.

2-(C_5H_4N)$\overline{CHNHC_6H_4S}$, HL^8. Pyridine-2-carbaldehyde (5 g, 0.05 mol) and 2-aminobenzenethiol (6.2 g, 0.05 mol) in ethanol (30 cm^3) were heated under reflux for 1 h, during which time the pale yellow colour of the final product developed. The solvent was then removed under vacuum to yield a yellow oil which was recrystallised from hot ethanol. The pale yellow crystals were filtered off at the pump and washed with cold methanol–ether. Yield 8.8 g (82%), m.p. 85 °C (Found: C, 68.1; H, 5.0; N, 12.7. $C_{12}H_{10}N_2S$ requires C, 67.3; H, 4.7; N, 13.1%);

ν(C–N) 1180s; ν(NH) 3165 (br), 1580s, 745s cm^{-1}; HPLC retention time = 9.6 min; *m/z* 214 (M^+) and 187 (M – HCN). NMR ($CDCl_3$): ^1H (60 MHz), δ 2.1 (1 H, s, CH), 5.4 (1 H, br, NH), 6.1–7.1 (7 H, m, aromatic protons) and 8.6 (1 H, m, *o*-pyridyl proton); ^{13}C (20 MHz), δ 127.27 (s, CS) and 69.9 (s, CHNH). λ_{max}(dmf) 315 and 251 nm.

Preparation of Metal Complexes.—The complexes of Fe, Co and Ni were prepared by treating a two-fold excess of the appropriate tridentate ligand precursor in ethanol with a solution of $FeCl_3$, air-oxidised $CoCl_2$ or $NiCl_2$ in the presence of triethylamine. The cationic iron and cobalt complexes were precipitated with an excess of $[NH_4][PF_6]$ or $Na[BPh_4]$. Analytical data for the complexes are given in Table 1.

Dichloro{2-[2-(diphenylphosphino)ethyliminomethyl]phenolato-N,O,P}*oxorhenate*(v). A solution of tetra-*n*-butylammonium tetrachlorooxorhenate(v)[25] (0.12 g, 0.2 mmol) in dry ethanol (10 cm^3) was added to a stirred solution of 2-[2-(diphenylphosphino)ethyliminomethyl]phenol (0.07 g, 0.2 mmol) in dry ethanol (10 cm^3) to give a dark brown-red solution. This was then heated under reflux on an oil-bath for 2 h. The volume of the solution was then reduced under vacuum to *ca.* 10 cm^3. On cooling to room temperature an olive-green solid deposited, which was filtered off, washed with ethanol (2 × 10 cm^3) and dried *in vacuo* (yield 0.06 g, 56%). ν(Re=O) 980s, ν(C=N) 1595w, 1618w cm^{-1} (Found: C, 41.8; H, 3.3; N, 2.3. $C_{21}H_{19}Cl_2NO_2Re$ requires C, 41.6; H, 3.15; N, 2.30%). NMR [$(CD_3)_2SO$]: ^1H, δ 1.01–1.06 (t, 2 H, PCH_2, $^3J_{HH}$ = 6.75), 3.39–3.47 (t, 2 H, NCH_2, $^3J_{HH}$ = 6.75 Hz), 6.88–7.3 (unresolved m, 3 H, phenol aryl protons), 7.32–7.85 (unresolved m, 11 H, phosphine protons and one phenol aryl proton) and 9.04 (s, 1 H, N=CH); ^{31}P, δ –4.3 (s, 1 P, Ph_2P) and 6.7 (s, 1 P, Ph_2P). *m/z* 570 (M – Cl).

Dichloro{2-[2-(diphenylphosphino)benzylideneamino]phenolato-N,O,P}*oxorhenate*(v). A solution of tetra-*n*-butylammonium tetrachlorooxorhenate (0.12 g, 0.2 mmol) in dry ethanol (10 cm^3) was added to a stirred solution of 2-[2-(diphenylphosphino)benzylideneamino]phenol (0.08 g, 0.2 mmol) in dry ethanol (10 cm^3) to give a dark brown solution. This was then heated under reflux on an oil-bath for 2 h. The volume of the solution was reduced under vacuum to *ca.* 10 cm^3. On cooling to room temperature a dark green solid deposited, which was filtered off, washed with ethanol (2 × 10 cm^3) and dried *in vacuo* (yield 0.11 g, 56%); ν(Re=O) 973s, ν(C=N) 1585w cm^{-1} (Found: C, 46.1; H, 3.4; N, 2.0. $C_{25}H_{19}Cl_2NO_2Re$ requires C, 45.9; H, 2.9; N, 2.1%). NMR [$(CD_3)_2SO$]: ^1H, δ 9.65 (s, 1 H, N=CH) and 7.82–6.65 (unresolved m, 18 H, aryl protons); ^{31}P, δ –9.11 (s, 1 P, Ph_2P) and 40.0 (s, 1 P, Ph_2P). *m/z* 618 (M – Cl).

Crystal Structure Determinations.—Full details of the data collection and structure determination appear in Table 7.

Additional material available from the Cambridge Crystallographic Data Centre comprises H-atom coordinates, thermal parameters and remaining bond lengths and angles.

Acknowledgements

We thank Dr. D. Povey at the University of Surrey for the structure determination of the complex $[CoL^1_2]^+$ and N. Barnard at the University of Essex for skilled assistance with the electrochemical measurements. We also gratefully acknowledge a gift of rhenium metal from Hermann Starck Gmb, Berlin and the SERC for the award of a studentship (to A. J. H.).

References

1 M. Otomo and K. Kadoma, *Bull. Chem. Soc. Jpn.*, 1973, **26**, 2421; Z. Holzbecher and H. van Trung, *Collect. Czech. Chem. Commun.*, 1976, **41**, 1506; K. Isagi and K. Isagi, *Nippon Kagaku Zashi*, 1967, **88**, 1292.
2 H. J. Banbery, W. Hussain, T. A. Hamor, C. J. Jones and J. A. McCleverty, *J. Chem. Soc., Dalton Trans.*, 1990, 657.
3 J. Bernstein and I. Izak, *J. Chem. Soc., Perkin Trans. 2*, 1976, 429 and refs. therein.
4 K. Nakamoto, *Infra-red and Raman Spectra of Inorganic Chemistry*, 5th edn., Wiley, London, 1988.
5 F. A. Cotton and G. Wilkinson, *Advanced Inorganic Chemistry*, 5th edn., Wiley, London, 1988.
6 D. N. Hendrickson, M. S. Haddad, W. D. Federer and M. W. Lynch, *Coord. Chem.*, 1980, **21**, 75.
7 H. Ohshio, Y. Maeda and Y. Takashima, *J. Radioanal. Nucl. Chem.*, 1985, **93**, 253.
8 H. K. B. Pandeya, R. Singh, C. Parkash and J. S. Baijal, *Solid State Commun.*, 1987, **64**, 801.
9 Y. Maeda, N. Tsutsumi and Y. Takashima, *Inorg. Chem.*, 1984, **23**, 2440.
10 C. K. Johnson, ORTEP, Report ORNL-5138, Oak Ridge National Laboratory, Oak Ridge, TN, 1976.
11 W. O. S. Motherwell and W. Clegg, PLUTO 78, University of Cambridge, 1978.
12 DIFABS, N. G. Walker and D. Stuart, *Acta Crystallogr., Sect. A*, 1983, **39**, 158.
13 G. M. Sheldrick, SHELX 80, Program for crystal structure determination, University of Cambridge, 1980.
14 MOLEN; An interactive structure solution procedure, Enraf-Nonius, Delft, 1990.
15 H. Nakai, M. Shiro, K. Eumzi, S. Sakata and T. Kubota, *Acta Crystallogr., Sect. B*, 1976, **32**, 1827.
16 J. Bernstein and A. J. Hagler, *J. Am. Chem. Soc.*, 1978, **100**, 673.
17 I. Bar and J. Bernstein, *Acta Crystallogr., Sect. B*, 1983, **39**, 266.
18 I. Bar and J. Bernstein, *Tetrahedron*, 1987, **43**, 1299.
19 A. Houlton, J. R. Miller, J. Silver, M. T. Ahmet, T. L. Axon, D. Bloor and G. H. Cross, *Inorg. Chim. Acta*, 1973, **205**, 67.
20 M. Y. Hamed, R. C. Hider and J. Silver, *Inorg. Chim. Acta*, 1982, **66**, 13.
21 D. Perrin and W. L. F. Armarego, *Purification of Laboratory Chemicals*, 3rd edn., Pergamon, London, 1988.
22 J. Corr, Ph.D. Thesis, University of North Carolina, 1967.
23 K. Issleib and H. Oehme, *Chem. Ber.*, 1967, **100**, 2685.
24 J. E. Hoots, T. B. Rauchfuss and D. A. Wrobleski, *Inorg. Chem. Synth.*, 1982, **21**, 175.
25 J. R. Dilworth, W. Hussain, A. J. Hutson, C. J. Jones and F. S. McQuillan, *Inorg. Synth.*, submitted for publication.

Received 28*th July* 1994; *Paper* 4/04645E